



## Pressure swing adsorption for the purification of Biogas

Rawnak Talmoudi<sup>\*</sup>, M H Chahbani<sup>a</sup>, Guy DeWeireld<sup>b</sup>, Pierre Billemont<sup>b</sup>,

<sup>\*</sup>Laboratoire de Recherche Génie des procédés et systèmes industriels, Ecole Nationale d'Ingénieurs de Gabès, Université de Gabès, Tunisie,

<sup>\*</sup>Talmoudirawnak@hotmail.com

<sup>a</sup>Institut Supérieur des Sciences Appliquées et de Technologie de Gabès, Rue Omar Ibn Elkhatab, Zrig, Gabès 6029, Tunisie,

chahbani.med\_hachemi@yahoo.com

<sup>b</sup>Faculté polytechnique de Mons, 20, place du Parc, 7000 Mons, Belgium

**Abstract:** Biogas consists of CH<sub>4</sub>, CO<sub>2</sub> with trace amounts of H<sub>2</sub>S and other impurities. In this study, the biogas was purified by Pressure Swing Adsorption (PSA). The equilibrium adsorption isotherms of biogas on the commercially Basolite A100 (Metal organic frameworks MOFs) adsorbent were investigated with a gravimetric sorption measurement apparatus at three temperatures (303, 313 and 323 K). The breakthrough curves were determined in a fixed bed unit involving feed of biogas at a pressure of 4 bars and temperature of 303 K. These experimental results were used for the design of PSA cycles for the recovery of CH<sub>4</sub>. The performances of these PSA cycles were evaluated by ASPEN ADSORPTION software.

**Key words:** Biogas, adsorption, equilibria, breakthrough curve, Basolite A100, PSA.

### 1. Introduction

Biogas is a valuable renewable energy carrier. It can be exploited directly as a fuel or as a raw material for the production of synthesis gas and/or hydrogen. Biogas is produced by conversion of organic matters using anaerobic digestion in several industrial processes as sewage treatment, landfills, cleaning of organic industrial waste streams and digestion of organic waste [1]. Depending on the origin of the organic matters and the used process, the composition of the produced gas mixture can vary. It is mainly composed of CH<sub>4</sub> (40–75%) and CO<sub>2</sub> (15–60%) but other compounds can be found in some quite important concentrations as H<sub>2</sub>S (5–20,000 ppm) and H<sub>2</sub>O (0–10%) or in trace concentrations (volatile organic compounds (VOC), NH<sub>3</sub>, N<sub>2</sub>, O<sub>2</sub>, CO, etc.).

The presence of CO<sub>2</sub> in important concentration leads to a decrease of the gas calorific value. The H<sub>2</sub>S, even in low concentration, is a toxic compound and can induce corrosion and acidic rains by the formation of SO<sub>2</sub> and SO<sub>3</sub> during the combustion of the biogas [2].

The most important biogas upgrading techniques are scrubbing with water or other physical solvent, chemical scrubbing, membranes and Pressure Swing Adsorption (PSA).

PSA is a well-known separation technique, which has been in practice for at least 40 years. The PSA based separation is considered as a feasible technology to be employed in natural gas and biogas upgrade due to its high energy efficiency, its simplicity, low capital investment cost, and ease of control.

The content of the impurities, such as CO<sub>2</sub>, H<sub>2</sub>S that must be stripped off in natural gas depends on its origin, and frequently has important variations even in a single region.

The design of PSA depends strongly on the properties of the adsorbent: adsorption loading and diffusion, thermal effects, etc. The adsorption separation process involves two principal steps: adsorption and desorption. High pressure during adsorption and the low pressure during desorption are the basic principles of component separation by PSA [3].

Besides these classical porous materials, the relatively new class of crystalline porous materials Metal-Organic Frameworks (MOFs) like Basolite A100 are attracting a great attention in large-scale carbon dioxide and hydrogen sulfide separations [4].

In this study, after evaluation the experimental equilibrium data for CO<sub>2</sub>/CH<sub>4</sub>/H<sub>2</sub>S on Basolites A100, an adsorption column performing the CH<sub>4</sub>, CO<sub>2</sub>, H<sub>2</sub>S separation with the Basolite A100 is simulated. The simulated results are compared with an experimental breakthrough curve. As this comparison is conclusive, a complete Pressure Swing Adsorption process PSA (one bed) allowing to produce CH<sub>4</sub> containing low concentrations of

CO<sub>2</sub> and H<sub>2</sub>S is finally simulated by ASPEN ADSORPTION. The recovery and purity of CH<sub>4</sub> were determined as 97,32% and 26%.

## 2. Experimental

One of MOFs family was used to measure pure adsorption isotherms of CH<sub>4</sub>, CO<sub>2</sub> and H<sub>2</sub>S. The commercially Basolite A100 is produced by BASF. This microporous material is consists of octahedral AlO<sub>4</sub>(OH)<sub>2</sub> units connected through 1,4-benzenedicarboxylate ligands. Its exchange surface according to the model of BET is in the range 1100-1500 m<sup>2</sup> / g [5,6].

The measurement of adsorption equilibrium isotherms of CH<sub>4</sub>, CO<sub>2</sub> and H<sub>2</sub>S was performed with a gravimetric method in a magnetic suspension microbalance (Rubotherm, Germany), refer to figure 1 for a Gravimetric set-up for adsorption measurement of pure gas on pourous materials.

This unit measures a succession of variations of a mass of a sample of adsorbent under different pressures in the system at a controlled temperature. The mass of adsorbent is weighed in a basket suspended by a permanent magnet through an electromagnet. The basket is placed in an adsorption cell operating at a range from vacuum to 15 MPa and at temperature range varying from 233 to 673 K [7].

Basolite A100 was activated at 200 C in a vacuum for 12 hours, whereas 1 was activated in a vacuum at ambient temperature for 48 hours.

Figure 2 shows scheme of a schematic representation of the adsorption column. Breakthrough curves were carried out using an adsorption column was able to operate with gas mixtures of three components and at flow rate from 0.2 to 10 NI min<sup>-1</sup>.

The appropriate gas mixture mole fraction 60% CH<sub>4</sub>, 39,5% CO<sub>2</sub> and 0,5% H<sub>2</sub>S was fed into the column of 50 cm high at 4 bar pressure and at a temperature of 303 K. The properties of the fixed-bed used in breakthrough curves experiments are presented in Table 1.

This column was surrounded by a double envelope in which water circulates in order to maintain the temperature of the column constant during the measurements. The water circulation was provided by a bath Alpha R8 and three thermocouples are placed within the column for measuring the temperature. The effluent gas flow analysis is performed using a mass spectrometer (MS), it allows to follow the variation of the concentrations of biogas components (CH<sub>4</sub>, CO<sub>2</sub>, H<sub>2</sub>S) with time.

The breakthrough curves performed after regeneration of the adsorbent under vacuum and at a precise temperature, flow rates necessary to obtain the desired gas concentrations are determined. , and we were realized the experience with recorded instructions.

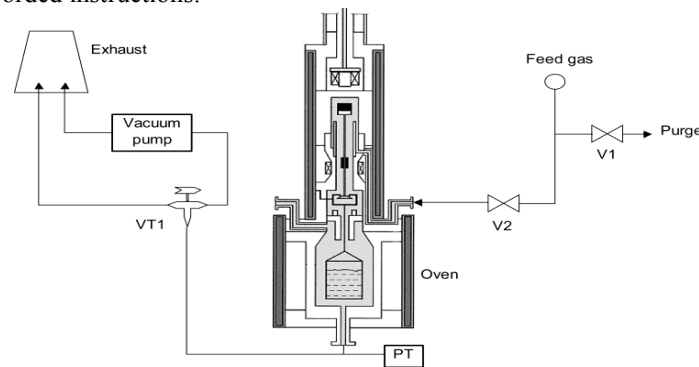


Figure 1 : Gravimetric set-up for adsorption measurement of pure gas on porous materials.

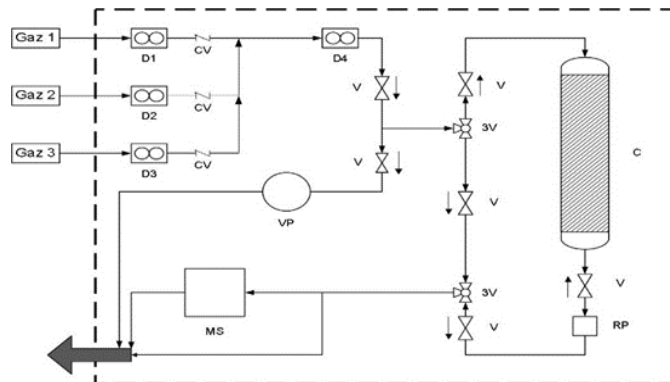


Figure 2: A schematic representation of the adsorption column

## 2. Modeling and simulation

### 2.1. Adsorption equilibrium

The multicomponent extension of the Langmuir model [8] was used to predict adsorption isotherms of CH<sub>4</sub>, CO<sub>2</sub> and H<sub>2</sub>S based on parameters obtained from pure component. The adsorption model parameters listed in Table 1.

Table 1 : Parameters of extended Langmuir model for the adsorption equilibrium of CH<sub>4</sub> CO<sub>2</sub> and H<sub>2</sub>S on Basolite A100

Gas	q <sub>m,i</sub> mol.kg <sup>-1</sup>	b bar <sup>-1</sup>
CH <sub>4</sub>	3,9	0,132
CO <sub>2</sub>	5,62	0,398
H <sub>2</sub> S	6,96	0,942

### 2.2. Fixed bed experiments

Figure 3 (a),(b) and (c) shows the breakthrough curves. Breakthrough experiments are a prerequisite to understand the adsorption dynamics and to test the validity of a theoretical approach by dynamic mathematical models. The breakthrough curve of each component is represented separately using an appropriate axis scale.

To build such mathematical model some assumptions must be made, such as: ideal gas behavior for the gas phase, constant void fraction, local pressure drop following Ergun equation, absence of temperature gradients within the solid particle, and that the column wall only interchanges energy with the gas phase and the external environment [8].

Kinetics of adsorption on basolite A100 was described by LDF (linear driving force) approximation for diffusion and mass transfer within a particle [10]. The mathematical models and all parameters for simulate the adsorption step is detailed in table 3.

The equations constituting the model were estimated according to correlations existing in literature .The correlations employed in the estimation of heat transfer parameters are summarized in Table 4 [8].

### 2.3. Cycle design

An Numerical modelling of a Pressure swing adsorption PSA cycle was simulated using the same PDE model than for the breakthrough curve simulations. The model was described in table 3 and 4. This model of breakthrough and PSA was solved numerically using Aspen Adsorption software. A schematic diagram of one bed of PSA cycle is shown in figure 4.

In this study, One bed of PSA cycle used to recover the methane was Skarstrom-type comprising pressurization with gas mixtures, an adsorption and production, a countercurrent blowdown step to regenerate the adsorbents and a purge with product steps .

The conditions to run one bed of PSA simulation were: mixture composition: 60%CH<sub>4</sub>, 39,5%CO<sub>2</sub> and 0,5% H<sub>2</sub>S. Feed pressure was kept constant at 4 bar while blowdown and purge were done at 1 bar. The duration of the different steps of the process are equal to 140 s for the adsorption and desorption steps, and 60 s for the pressurization and depressurization steps.

The performance of the PSA cycle was evaluated according two parameters: purity and recovery of product (methane) [9]. They are defined by

$$Purity = \frac{\int_0^{t_{feed}} C_{CH_4} \nu \Big|_{z=L} dt}{\left( \int_0^{t_{feed}} C_{CH_4} \nu \Big|_{z=L} dt + \int_0^{t_{feed}} C_{CO_2} \nu \Big|_{z=L} dt + \int_0^{t_{feed}} C_{H_2S} \nu \Big|_{z=L} dt \right)} \quad (1)$$

$$\text{Recovery} = \frac{\int_0^{t_{feed}} C_{CH_4} v \Big|_{z=L} dt - \int_0^{t_{purge}} C_{CH_4} v \Big|_{z=L} dt}{\int_0^{t_{feed}} C_{CH_4} v \Big|_{z=0} dt} \quad (2)$$

Where  $t_{feed}$  and  $t_{purge}$  are feed and purge times, respectively.

Table 2 : Properties of the column used and the Physical properties of adsorbent and of the fixed-bed breakthrough curves on Basolite A100

Parameter	Value	Unit
Bed porosity ( $\epsilon$ )	0,382	-
Bed length	0,5	m
Bed diameter	0,0217	m
Column wall specific heat	500	J kg <sup>-1</sup> K <sup>-1</sup>
Column wall density	7990	Kg.m <sup>-3</sup>
Particle diameter	0,00343	m
Adsorbent specific heat capacity	1264	J kg <sup>-1</sup> K <sup>-1</sup>
Particle density	497	Kg.m <sup>-3</sup>

Table 3 : Mathematical model for fixed bed and PSA used for methane-carbon dioxide-hydrogen sulfide separation

Continuity equation	$\frac{\partial C}{\partial t} + \frac{\partial(v_g C)}{\partial Z} + \frac{(1-\epsilon)}{\epsilon} \frac{\partial q}{\partial t} = -D_z \frac{\partial^2 C}{\partial Z^2}$
Ergun equation	$\frac{\partial P}{\partial Z} = 150 \frac{(1-\epsilon)^2}{\epsilon^2 d_p^2} \mu v_g + 1.75 \frac{(1-\epsilon)}{\epsilon d_p} \rho_g v_g^2$
linear driving force (LDF)	$\frac{\partial q}{\partial t} = k_m (q^* - q) = \frac{15D_c}{r_p^2} (q^* - q)$
Extended Langmuir model	$q = q_m \frac{b_j P}{1 + \sum b_j P}$ , $b = b_o \exp \frac{E}{T}$
Heat balance	$\epsilon a_f \rho_g C_{pg} \frac{\partial T_g}{\partial t} - \epsilon a_f k_g \frac{\partial T_g}{\partial Z^2} = -\epsilon a_f \rho_g C_{pg} v_g \frac{\partial T_g}{\partial Z} + a_s h_{sg} (T_s - T_g) + \epsilon P_i h_{wg} (T_w - T_g)$
Sorbent heat Balance	$a_f \rho_s C_{ps} \epsilon \frac{\partial T_g}{\partial t} - a_s k_s \frac{\partial^2 T_s}{\partial Z^2} = a_s h_{sg} (T_g - T_s) - a_f \frac{\partial q}{\partial t}$
Column heat Balance	$a_w \rho_w C_{pw} \frac{\partial T_w}{\partial t} - a_w k_w \frac{\partial^2 T_w}{\partial Z^2} = \epsilon_w P_i h_{wg} v_g (T_g - T_w) + P_o h_{wa} (T_g - T_w)$

Table 4 : Correlations used for estimation of heat transfer parameters

Film heat transfer (Ruthven,1984)	$Nu = (2.0 + 1.1 Re^{0.6} Pr^{1/3})$ , $Nu = \frac{k_g d_p}{\lambda_f}$ , $Pr = \frac{\mu_g C_{pg}}{\lambda_f}$ , $Re = \frac{\rho_g v_g d_p}{\mu_f}$
heat transfer between gas and wall (Molerus,1993)	$Nu = (3.66^3 + 1.61^3 Pe_{w,i} \frac{d_p}{L})^{1/3}$ , $Pe_{w,i} = \frac{\rho_g v_g C_{pg} d_p^*}{\lambda_f}$ , $d_p^* = \frac{2\epsilon}{3(1-\epsilon)} d_p$
heat transfer between the ambient and the wall(Kreith and Bohn,1993)	$Nu = (0.023 Re^{0.8} Pr^{1/3})$ , $Nu = \frac{k_{we} D_h}{\lambda_{water}}$ , $Pr = \frac{\mu_{water} C_{p,water}}{\lambda_{water}}$ , $Re = \frac{\rho_{water} v_{water} D_h}{\mu_{water}}$

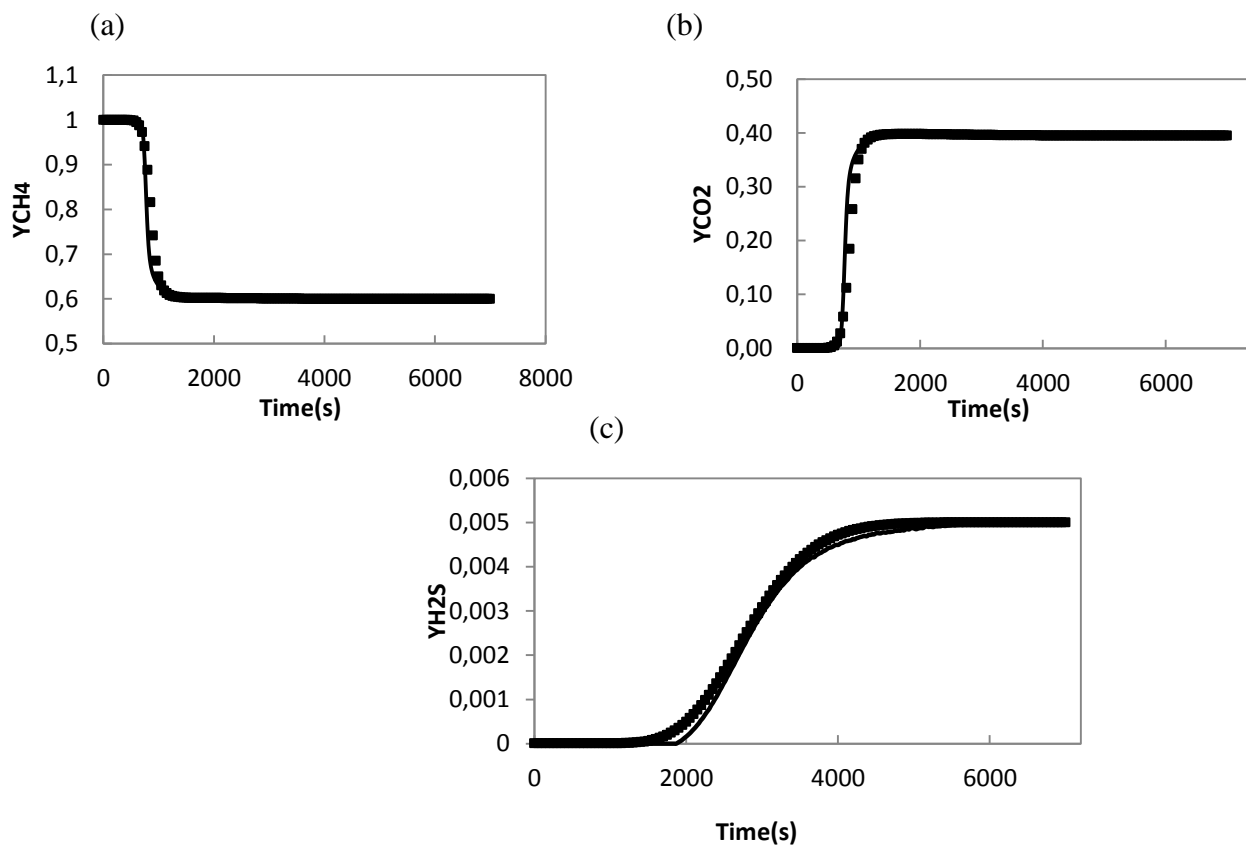


Figure 3: Breakthrough curve at 4 bars and 303 K for a mixture of 5 % H<sub>2</sub>S, 39.5% CO<sub>2</sub> and 60% CH<sub>4</sub> over a bed of Basolite A100 initially full of methane; Filled Solid lines and symbols represent curve data fittings experimental and using Aspen adsorption respectively.

I	II	III	IV
Adsorption 4 bar 60% CH <sub>4</sub> ; 39,5% CO <sub>2</sub> ; 5% H <sub>2</sub> S	Blowdown 4bar → 1bar	Purge 1 bar 100% CH <sub>4</sub>	Pressurization 1 bar → 4 bar

Figure 4 : One bed of Cycle sequence used in PSA simulation

### 3. Results and discussion

The breakthrough experimental results agree well with the predicted results, this shows clearly the reliability of the mathematical model to simulate the adsorption process. Methane, more weakly adsorbed, was the first component detected at the bed outlet after 500 s and carbon dioxide, was the second component detected after 650 s and hydrogen sulfide, more strongly adsorbed, is not detected before 1500 s. For an initial period of 500 s, only methane is exiting the bed, which corroborates the ability of Basolite A100 to separate concentrated carbon dioxide/methane/ hydrogen sulfide mixtures.

The simulation of breakthrough curve has to be mentioned that these breakthrough curves are useful to determine the mass transfer coefficient  $k_m$ , obtained as a fitting parameter from these curves and then used in all the PSA simulations. The mass transfer coefficient of  $\text{CH}_4$ ,  $\text{CO}_2$  and  $\text{H}_2\text{S}$  are, respectively, 0,8; 5 and 0,08 (1/s).

The steady state was obtained after 15 cycle. In Figure 5 we show the pressure history at the outlet of the column for cycle 15 and the evolution of the  $\text{CH}_4$  mole fraction in the end of adsorption step.

During the adsorption step the  $\text{CO}_2$  front moves forward in the bed and the step is stopped before the front breakthrough the bed.

The results of purity confirm the possibility of using the Basolite A100 for the enrichment of biogas containing  $\text{CH}_4$ ,  $\text{CO}_2$  and  $\text{H}_2\text{S}$  (respectively 60%, 39,5% and 0,5%) to obtain a flow containing at least 97,32 % of  $\text{CH}_4$  with a product recovery of 26%.

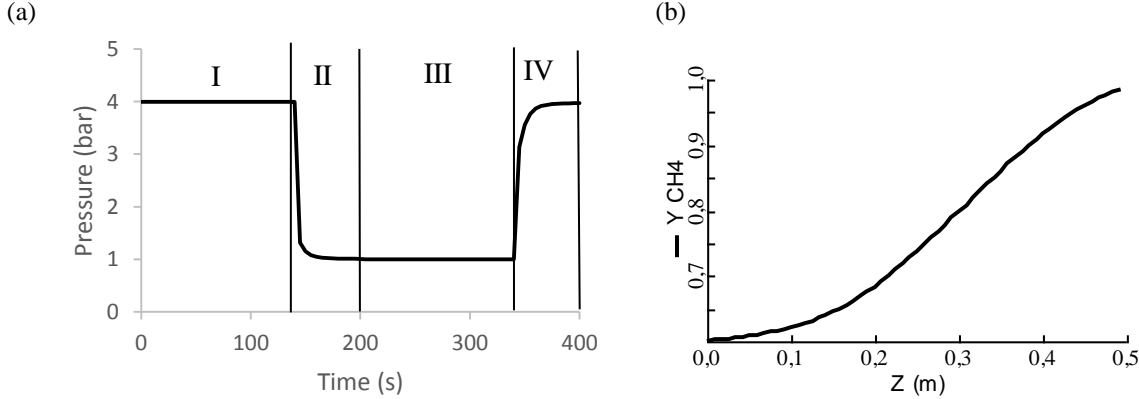


Figure. 5. One column simulation of PSA for  $\text{CH}_4$ – $\text{CO}_2$ – $\text{H}_2\text{S}$  separation using Basolite A100. Cycle scheme is shown in Fig. 4 and operating conditions in Table 2. Results presented are : (a) pressure history of dynamic cycle used in simulation for PSA Cycle 15 and (b) the evolution of the  $\text{CH}_4$  mole fraction in the end of adsorption step exiting the column.

## Conclusion

The first part of this study, a sample of Basolite A100 was successfully evaluated for the upgrade of methane by Pressure Swing Adsorption. The second part, it consists in performing the breakthrough curve of the limiting separation according to the selectivity values ( $\text{CO}_2/\text{CH}_4/\text{H}_2\text{S}$ ). The results show that this separation is applicable. Moreover, the simulated curves are in good agreement with the experimental curves.

The last step of the study is the simulation of a complete PSA process. In the simulation conditions, the produced flow contains at least 97,32% of  $\text{CH}_4$ . So, the simulation shows the feasibility of the separation of  $\text{CO}_2$  and  $\text{H}_2\text{S}$  from  $\text{CH}_4$  by such a process using the Basolite A100 as adsorbent.

## Nomenclature

### Symbole

$a_f$	superficial free flow area, $m^2$	$D_h$	hydraulic diameter, $m$
$a_w$	column cross-sectional area, $m^2$	$D_z$	axial dispersion coefficient, $m^2 \cdot s^{-1}$
$b$	langmuir equation parameter, $bar^{-1}$	$E$	langmuir equation parameter
$b_o$	langmuir equation parameter, $bar^{-1}$	$h_{sg}$	sorbent to gas heat transfer coefficient, $W m^{-2} K^{-1}$
$C$	concentration, $mol \cdot m^{-3}$	$h_{wg}$	column wall to gas heat transfer coefficient, $W m^{-2} K^{-1}$
$C_{pg}$	gas heat capacity, $J kg^{-1} K^{-1}$	$K^1$	
$C_{ps}$	sorbent heat capacity, $J kg^{-1} K^{-1}$	$h_{wa}$	column wall to water heat transfer coefficient, $W m^{-2} K^{-1}$
$C_{pw}$	column wall heat capacity, $J kg^{-1} K^{-1}$	$k_g$	gas conduction, $W m^{-1} K^{-1}$
$C_{p,water}$	water heat capacity, $J kg^{-1} K^{-1}$	$k_m$	mass transfer coefficient, $s^{-1}$
$d_p$	particule diameter, $m$	$k_s$	sorbent conduction, $W m^{-1} K^{-1}$
$d_p^*$	equivalent particle diameter, $m$	$k_w$	column wall conduction, $W m^{-1} K^{-1}$
		$k_{we}$	column wall and water conduction coefficient,

	$W m^{-1} K^{-1}$
$L$	bed height, $m$
$q$	average adsorbed concentration, $mol.m^{-3}$
$q^*$	equilibrium adsorption concentration, $mol.m^{-3}$
$q_{m,i}$	adsorption capacity of the amount, $mol.kg^{-1}$
$P$	partial pressure, $Pa$
$P_i$	column inner perimeter, $m^2$
$P_o$	column outer perimeter, $m^2$
$r_p$	pellet radius, $m$
$t$	time, $s$
$T_g$	gas temperature, $K$
$T_s$	sorbent temperature, $K$
$T_w$	column wall water temperature, $K$
$Z$	axial coordinate, $m$
$\partial H$	differential heat of adsorption, $kJ mol^{-1}$

Symboles grecs	
$\varepsilon$	void fraction
$\mu$	dynamic viscosity, $Pa s$
$\mu_{water}$	water dynamic viscosity, $Pa s$
$U_g$	interstitial velocity, $m s^{-1}$
$U_{water}$	interstitial velocity in column of water, $m s^{-1}$
$\rho_g$	gas density, $kg m^{-3}$
$\rho_s$	sorbent density, $kg m^{-3}$
$\rho_w$	column wall density, $kg m^{-3}$
$\rho_{water}$	water density, $kg m^{-3}$
$\lambda_f$	heat axial dispersion coefficient, $W m^{-2} K^{-1}$
$\lambda_{water}$	water axial dispersion coefficient, $W m^{-2} K^{-1}$

### Références

- [1] O. Jönsson, E. Polman, J.K. Jensen, R. Eklund, H. Schyl, S. Ivarsson, in: World Gas Conference Tokyo 2003, International Gas Union, Oslo, Norway, 2003, pp. 9–18.
- [2] E. Ryckebosch, M. Drouillon, H. Vervaeren, Biomass Bioenergy 35 (2011) 1633–1645.
- [3] D.R. Pande, C. Fabiani, Gas Sep. Purif. 3 (1989) 143–147.
- [4] A.R. Millward, O.M. Yaghi, J. Am. Chem. Soc. 127 (2005) 17998–17999.
- [5] Alhamami M., Doan H., Cheng C., A review on breathing behaviors of metal-Organic-Frameworks (MOFs) for gas adsorption. Materials 2014, pp 3198-3250.
- [6] Christopher H and al., Engineering the Optical Response of the Titanium-MIL-125 Metal– Organic Framework through Ligand Functionalization. Journal of the American chemical society 2013, pp 10942–45.
- [7] Paschke T., Dreisbach F., ECBM: Gravimetric Adsorption Measurements Under Realistic Conditions Using Teledyne Isco Syringe Pumps, Rubotherm GmbH, Bochum, Germany.
- [8] Ruthven, D. M., Principles of Adsorption and Adsorption Processes, John Wiley & Sons, New York 1984.
- [9] A.C José and al., Separation of n/iso paraffins by PSA. J. separation and purification technology. 20(2000) 97-110.
- [10] Lei M., Vallires C., Grevillot G., Latifi M.A. Modeling and Simulation of a Thermal Swing Adsorption Process for CO2 Capture and Recovery. Industrial and Engineering Chemistry Research 2013, pp 7526–33.

**Monastir - Tunisie**